

Dynamic and Static Pull-in instability of electrostatically actuated nano/micro membranes under the effects of Casimir force and squeezed film damping

Kia Dastani, Mahdi Moghimi Zand*

Mechanical Engineering Department, College of Engineering, University of Tehran, Tehran, Iran

Received: 13 Aug. 2016 , Accepted: 2 Nov. 2016

Abstract

In the current study, the effects of Casimir force and squeeze film damping on pull-in instability and dynamic behavior of electrostatically actuated nano and micro electromechanical systems are investigated separately. Linear elastic membrane theory is used to model the static and dynamic behavior of the system for strip, annular and disk geometries. Squeeze film damping is modeled using nonlinear Reynolds equation. Both equation of motion and nonlinear Reynolds equation are first nondimensionalized, and then discretized and solved by means of finite element method. Static pull-in analysis is performed and validated by previous researches, and then dynamic pull-in values are investigated and compared with static pull-in parameters. In the next step, the effect of squeeze film damping, ambient pressure and Casimir force on the system dynamics is studied. Results show significant effect of Casimir force and squeeze film damping on the system behavior which is considerable for fabrication and design.

Keywords: MEMS, NEMS, Pull-in instability, Squeeze film damping, Casimir force, Linear elastic membrane, FEM

1. Introduction

Electrostatically actuated microelectromechanical systems are widely used these days in many applications such as microswitches, micromirrors, micro resonators, micro valves, sensors and etc. due to high reliability, low energy consumption, good durability and their small size. The most important phenomena happens under the effect of electrostatic actuation is pull-in instability, which has been introduced by Nathanson et al. [1] and Taylor [2]. Most of the electrostatically actuated systems are made up of a conductive deformable electrode suspended over a rigid substrate as shown in Fig 1. An applied electric

voltage between two electrodes results in the deflection of the deformable electrode. Therefore, system capacitance is changed and measuring this change is the basis of electrostatic sensors performance like accelerometers. When the electrostatic force exceeds the elastic restoring force of the structure, pull-in instability occurs and two electrodes snap together and subsequently the device collapses. Therefore, the applied voltage has an upper limit which is called pull-in voltage. Calculating pull-in voltages is extremely important in design and fabrication process of MEMS. In most of previous researches pull-in instability has been studied statically. Batra et al have studied static pull-in instability of electrostatically-actuated microelectromechanical systems considering

* Corresponding Author. Tel.: +98-21-61114807, Fax: +98-21-88013029
Email Address: mahdimoghimi@ut.ac.ir

the effect of Casimir force [3]. Moeenfarid et al have investigated the effect of Casimir force on the static behavior and pull-in characteristics of nano/micro-mirrors under capillary forces [4]. Dequesnes et al have studied the static pull-in characteristics of several nanotube electromechanical switches [5]. Tilimans et al have investigated the static pull-in parameters of electrostatically driven vacuum-encapsulated polysilicon resonators [6]. Sadeghian has investigated the surface effects, specifically residual surface stress and surface elasticity, on the electrostatic pull-in instability of micro and nano-scale cantilevers as well as double-clamped beams [7]. When the rate of voltage variation is insignificant, it is sufficient to study the pull-in instability statically [10]. When the rate of voltage variation is not negligible, the inertia effect must be considered and behavior of the system has to be studied dynamically [10]. In this situation the upper limit of voltage is called dynamic pull-in voltage [10]. Alsaleem et al have presented modeling, analysis and experimental investigation for the dynamic pull-in instability in resonators [8]. Krylov and Maimon have studied pull-in dynamics of an elastic beam actuated by continuously distributed electrostatic force [9]. Moghimi Zand and Ahmadian have investigated the effect of intermolecular forces on the dynamic pull-in instability of electrostatically actuated beams [10]. Moghimi Zand and Ahmadian have also studied dynamic pull-in instability of microsystems using homotopy analysis [11]. Studying dynamic behavior and vibrations of microsystems is important in design process, because many microsystems work on the basis of vibrations. Therefore, several researches has been analyzed the dynamic behavior and vibrations of MEMS and NEMS. Daneshpajoooh and Moghimi Zand have studied oscillatory behavior of initially curved micro/nano systems under electrostatic actuation [12]. Moghimi Zand et al have also investigated nonlinear vibrations of microbeams under suddenly applied voltages [13]. Nayfeh and Younis have presented an analysis and simulation for the dynamics of electrically actuated microbeams [14]. Moghimi Zand and Ahmadian have studied the vibrational behavior of electrostatically actuated microstructures [15].

When the system dimension decreases from macro to micro, the effect of damping becomes significant and should be considered in modeling and design process. The most important type of energy losses in microsystems is fluid losses and the effect of squeeze film damping. Fluid effects are generally divided into shear (Couette) damping, where the fluid velocity is parallel to the electrode and squeeze film, where the velocity is normal to the electrode [16]. Several authors have studied the effect of squeeze film damping on the dynamic behavior of MEMS and NEMS [17-20]. Some numerical and analytical models

have been used to model fluid losses in microsystems. A common way to model the squeeze film damping is to use Reynolds equation which is valid when (a) the gap height is much smaller than the length of electrodes; (b) the motion is sufficiently slow and the unsteadiness can be neglected; (c) the gas is ideal; (d) the system is isothermal [21]. Tajalli et al have used Reynolds equation to model the squeeze film damping in order to investigate dynamic behavior of a coupled domain microstructure [22]. Bao et al have modeled the squeeze film damping effect using a modified Reynolds equation [23]. With the assumption of small pressure variation and small displacement, squeeze film damping can be modeled using linear Poisson equation, a simplified Navier-Stokes equation instead of nonlinear Reynolds equation [24]. Starr has modeled squeeze film damping in accelerometers using Poisson equation [25]. Another way to model squeeze film damping is to apply molecular dynamics approach [26]. Hutcherson and Ye have also investigated the effect of squeeze film on the micromachined mechanical resonators by means of molecular dynamics simulations [27].

By the decrease in device dimensions from microscale to nanoscale, the effect of intermolecular forces such as Casimir and Van der Waals forces should be considered [3]. Casimir force is the attraction of two uncharged bodies. When the size of the system is sufficiently small, Casimir force can cause static pull-in and collapse of the system. So it is important to consider this force in design process. Moghimi Zand and Ahmadian have studied the influence of Casimir force on the dynamic pull-in instability of microbeams [10]. Alipour et al have investigated the effect of intermolecular forces on the behavior of nanotubes [28]. Koochi et al have studied the effect of the Casimir attraction on pull-in instability of beam-type NEMS theoretically [29]. Keivani et al have studied the pull-in instability of the cantilever paddle-type and double-sided sensors in the Casimir regime under the acceleration [30]. In some other researches, the influences of Casimir force on the nonlinear behavior of nanoscale electrostatic actuators have been studied [31-35].

In some recent researches, the effect of small scale and intermolecular forces on the behavior of systems have been studied [36, 37]. Kanani et al have modeled the size dependent pull-in instability of cantilever nano-switch immersed in ionic liquid electrolytes using strain gradient theory [38].

In most previous researches, beam theories have been used to model the static and dynamic behavior of micro and nano electromechanical systems. In few papers, plate theories such as CPT and FSDT have

been used for this purpose. Saghir and Younis have presented and compared different approaches to develop reduced-order models for the nonlinear von-Karman rectangular microplates actuated by nonlinear electrostatic forces for the purpose of studying static and dynamic behavior of the plate under small and large actuation forces [39]. Batra et al have modeled microsystems by means of linear elastic membrane theory to study static pull-in instability [3]. Also Serry et al have studied Casimir effect in the static deflection and stiction of membrane strips in MEMS [40]. However, the dynamic pull-in instability in micro/nano systems has not been modeled using linear elastic membranes yet.

The main idea of the present research is to model micro and nanoelectromechanical systems using membrane theory. In this paper, the effect of Casimir force and squeeze film damping on the dynamic behavior of micro and nano devices and the influence of Casimir force on dynamic pull-in instability of systems is studied. For this purpose, linear elastic membrane theory is applied to model the deformable electrode. Three different geometries are considered: Strip, annular and disk electrodes. Nonlinear Reynolds equation is used to model squeeze film air damping. Finally, Finite element method is applied to solve the governing equations.

2. Problem formulation

In this research linear elastic membrane theory is applied to model the deformable electrode. Membranes could be considered a simplified plate which has negligible bending resistance and gravitational body forces are to be neglected. A primary indication of membrane dynamics is given by the ratio L/h falling between 80 and 100. To be considered a true membrane, a structure must satisfy the following conditions a) The boundaries are free from transverse shear forces and moments and Loads applied to the boundaries must lie in planes tangent to the middle surface. b) The normal displacements and rotations at the edges are unconstrained i.e. these edges can displace freely in the direction of the normal to the middle surface. c) A membrane must have a smoothly varying, continuous surface. d) The components of the surface and edge loads must also be smooth and continuous functions of the coordinates [41].

In the present research three sample geometries have been considered: a rectangular strip with the length L and the width $L/8$ which is clamped on smaller edges and other edges are free, the circular disk which is clamped along its periphery and the annular circular disk which its outer radius is L and inner radius is $L/10$ and is clamped on both inner and outer

perimeters. The schematic of microstructure is shown in Fig. 1.

The equation of motion based on linear elastic membrane theory in the presence of fluid is given by:

$$\rho \frac{\partial^2 w}{\partial t^2} - \sigma_0 h \left(\frac{\partial^2 w}{\partial x^2} + \frac{\partial^2 w}{\partial y^2} \right) = f_e + f_c + (P - P_0) \quad (1)$$

where w is deflection of electrode along z axis, ρ (kg/m^2) is the mass per unit of area of electrode, σ_0 is the tensile stress in the membrane, h is thickness, P is total fluid pressure and P_0 is the ambient pressure. f_e is the electrostatic force acting on electrode which can be simplified under the assumption of parallel plate and neglecting fringing field effect as [22]

$$f_e = -\frac{\epsilon_0 V^2}{2(g_0 + w)^2} \quad (2)$$

where ϵ_0 (F/m) is the vacuum permittivity, V is applied voltage between two electrodes and g_0 is initial gap.

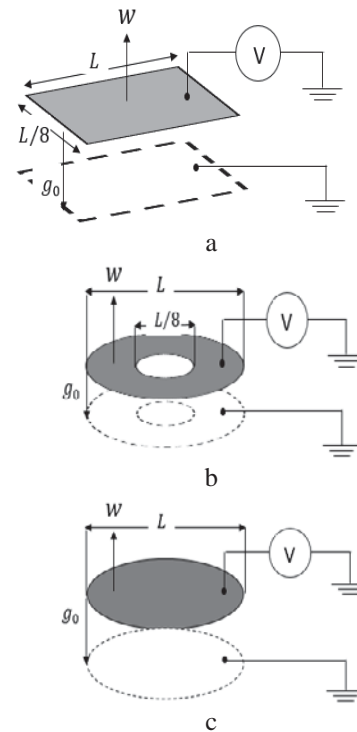


Fig 1. (a) strip (b) annular disk (c) strip Microstructures

In equation 1 f_c is the Casimir force which is given by Eq. 3 as [22]

$$f_c = -\frac{\bar{h}c\pi^2}{240(g_0 + w)^4} \quad (3)$$

where c is the speed of light in vacuum and \bar{h} is Plank's constant that is $6.62607004 \times 10^{-34} m^2kg/s$. As mentioned nonlinear compressible Reynolds equation

is applied to model the effect of fluid losses and squeeze film air. The applied Reynolds equation is [22]

$$\frac{\partial}{\partial x} \left(H^3 P \frac{\partial P}{\partial x} \right) + \frac{\partial}{\partial x} \left(H^3 P \frac{\partial P}{\partial x} \right) = 12\eta_{eff} \left(H \frac{\partial P}{\partial t} + P \frac{\partial H}{\partial t} \right) \quad (4)$$

where P is the total fluid pressure and H is the distance between to electrodes i.e. $H = g_0 + w$ and η_{eff} is the effective gas viscosity. Reynolds equation is valid under the assumption that gas can be treated as a continuum. The validity of this assumption depends on Knudsen number K_n defined as [19]

$$K_n = \frac{\lambda}{H} \quad (5)$$

where λ is molecular mean free path of gas. The flow is continuum when $K_n < 0.01$. Many MEMS devices operate under the condition that the flow is closer to noncontinuum regimes. In this situation effective viscosity coefficient η_{eff} should be used in Reynolds equation instead of viscosity. η_{eff} is calculated using Veijola equation as [42]

$$\eta_{eff} = \frac{\eta}{1 + 9.638K_n^{1.159}} \quad (6)$$

The pressure boundary conditions of Reynolds equation are expressed as $\frac{\partial P}{\partial x} = 0$ along clamped edges and $P = P_0$ on free edges. By utilizing following non-dimension parameters

$$\begin{aligned} \hat{x} &= \frac{x}{L}, \quad \hat{y} = \frac{y}{L}, \quad \hat{w} = \frac{w}{g_0}, \\ \hat{t} &= t \sqrt{\frac{\sigma_0}{\rho L^2}}, \quad \lambda = \frac{\epsilon_0 V^2 L^2}{2\sigma_0 h g_0^3}, \\ \mu &= \frac{\bar{h} c \pi^2 L^2}{240 \sigma_0 h g_0^5}, \quad \hat{P} = \frac{P L^2}{g h \sigma_0}, \quad \gamma = \frac{12 \eta_{eff} L^3}{g_0^3 \sqrt{h \sigma_0 \rho}} \end{aligned} \quad (7)$$

Non-dimensional form of equation of motion and Reynolds equation can be expressed as

$$\frac{\partial^2 \hat{w}}{\partial \hat{t}^2} - \frac{\partial^2 \hat{w}}{\partial \hat{x}^2} - \frac{\partial^2 \hat{w}}{\partial \hat{y}^2} = -\frac{\lambda}{(1 + \hat{w})^2} - \frac{\mu}{(1 + \hat{w})^4} + \hat{P} - \hat{P}_0 \quad (8)$$

$$\frac{\partial}{\partial \hat{x}} \left((1 + \hat{w})^3 \hat{P} \frac{\partial \hat{P}}{\partial \hat{x}} \right) + \frac{\partial}{\partial \hat{y}} \left((1 + \hat{w})^3 \hat{P} \frac{\partial \hat{P}}{\partial \hat{y}} \right) = \gamma \left((1 + \hat{w}) \frac{\partial \hat{P}}{\partial \hat{t}} + \hat{P} \frac{\partial \hat{w}}{\partial \hat{t}} \right) \quad (9)$$

3. Finite element modeling and computational algorithm

Finite element method is employed to discretize governing equations. Based on linear elastic membrane theory, variables w and P can be approximated using 4-node linear elements as

$$\hat{w}(x, y, t) = \sum_{i=1}^n W_i(t) \psi_i(x, y), \quad n = 4 \quad (10)$$

$$\hat{P}(x, y, t) = \sum_{i=1}^n P_i(t) \psi_i(x, y), \quad n = 4 \quad (11)$$

where W_i and P_i are nodal values of w and P and ψ_i are linear interpolation functions which in terms of element coordinates ζ and η are expressed as

$$\begin{pmatrix} \psi_1 \\ \psi_2 \\ \psi_3 \\ \psi_4 \end{pmatrix} = \frac{1}{4} \begin{pmatrix} (1 - \zeta)(1 - \eta) \\ (1 + \zeta)(1 - \eta) \\ (1 + \zeta)(1 + \eta) \\ (1 - \zeta)(1 + \eta) \end{pmatrix} \quad (12)$$

By substituting Eq. 10 and Eq. 11 in the weak form of motion and Reynolds equations, semi-discrete finite element model can be developed as

$$[M^e] \left\{ \overset{\cdot}{W} \right\}^{(n+1)} + [K^e] \{W\}^{(n+1)} = \{f^e\}^{(n)} \quad (13)$$

where n is the iteration number and $[M^e]$, $[K^e]$ and $\{f^e\}$ are the mass matrix, stiffness matrix and force vector respectively which are defined as

$$M_{ij}^e = \iint_{\Omega_e} \psi_i \psi_j dA \quad (14)$$

$$K_{ij}^e = \iint_{\Omega_e} (\psi_{i,x} \psi_{j,x} + \psi_{i,y} \psi_{j,y}) dA \quad (15)$$

$$f_j^e = Q_j^e + \iint_{\Omega_e} \left(-\frac{\lambda}{(1 + \hat{w})^2} - \frac{\mu}{(1 + \hat{w})^4} \right) \psi_j dA \quad (16)$$

where Q_j^e are nodal reactions. Semi-discrete finite element form of Reynolds equation can be expressed as

$$[C^p]^{(n)} \{\dot{P}\}^{(n+1)} + [K^p]^{(n)} \{P\}^{(n+1)} = -[C^w]^{(n)} \{\dot{W}\}^{(n)} + \{Q^s\} \quad (17)$$

where n is the iteration number. The detailed components of matrices $[C^p]$, $[K^p]$, $[C^w]$ and vector $\{Q^s\}$ are expressed as

$$K_{ij}^p = \iint_{\Omega_e} (\psi_{i,x} \psi_{j,x} + \psi_{i,y} \psi_{j,y}) \times P^{(n)} (1 + \hat{w}^{(n)})^3 dA \quad (18)$$

$$C_{ij}^p = \gamma \iint_{\Omega_e} \psi_i \psi_j (1 + \hat{w}^{(n)}) dA \quad (19)$$

$$C_{ij}^w = \gamma \iint_{\Omega_e} \psi_i \psi_j \hat{P}^{(n)} dA \quad (20)$$

$$Q_i^s = \int_{\Gamma_e} \psi_i P^{(n)} (1 + \hat{w}^{(n)})^3 (\nabla P^{(n+1)} \cdot \vec{ds}) \quad (21)$$

Fully discretized form of equation of motion has been developed by means of Newmark time discretization (trapezoidal rule). Fully discretized form of Reynolds equation is developed as

$$[\tilde{K}]^{(n)} \{P\}^{(n+1)} = \{\tilde{f}\}^{(n)} \quad (22)$$

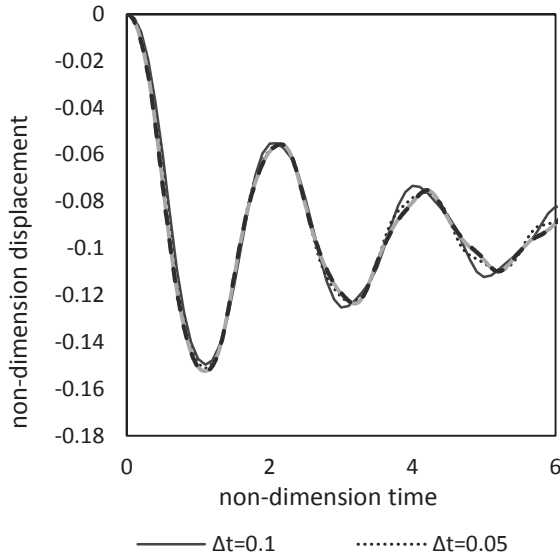
where $[\tilde{K}]$ and $\{\tilde{f}\}$ can be obtained by applying forward time difference for \dot{P} and backward time difference for \dot{W} as

$$[\tilde{K}]^{(n)} = \frac{1}{\Delta t} [C^p]^{(n)} + [K^p]^{(n)} \quad (23)$$

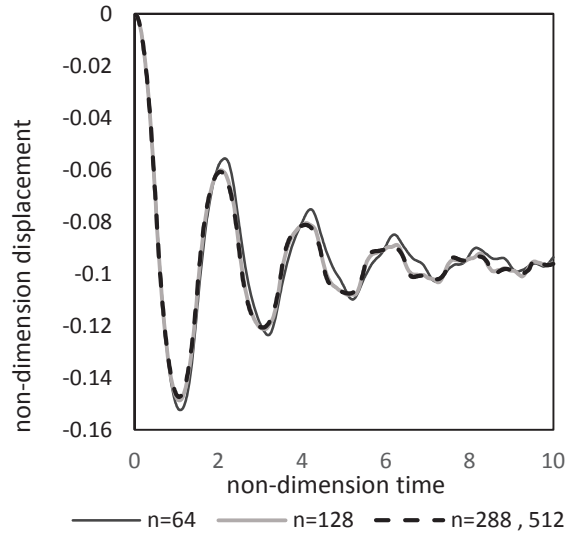
$$\{\tilde{f}\}^{(n)} = \frac{1}{\Delta t} \left([C^p]^{(n)} \{P\}^{(n)} - [C^w]^{(n)} (\{W\}^{(n)} - \{W\}^{(n-1)}) \right) \quad (24)$$

where Δt is time step. In each time step first equation of motion is solved. The Eq. 22 is solved using deflection calculated from Eq. 13. The numerical integration over element area is performed using Gaussian quadrature method.

4. Results and discussion



a



b

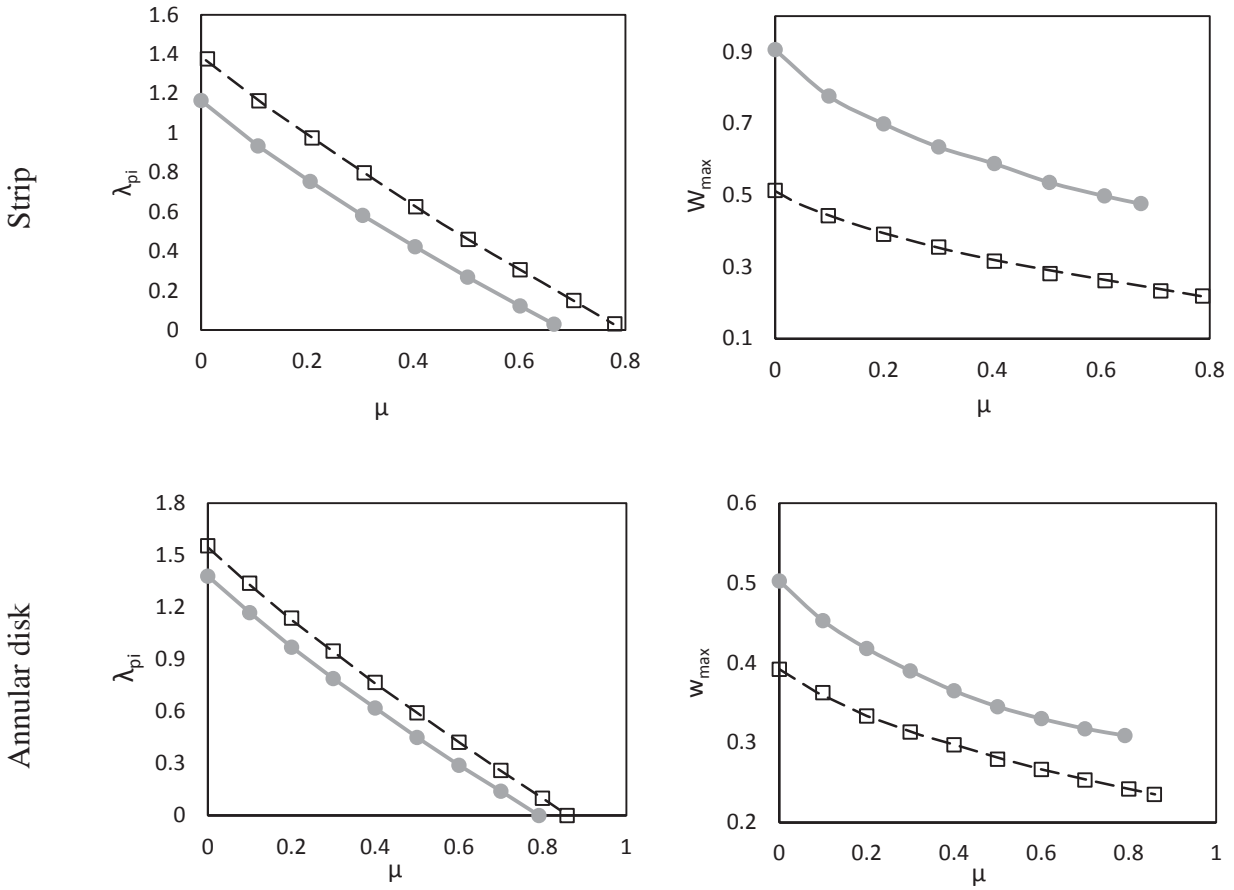
Fig. 2. Midpoint deflection time history for (a) various time increments and (b) different number of elements. For $\mu = 0$, $\gamma = 1000$ and $\hat{P}_0 = 5$

In order to study dynamic behavior of microsystem, first convergence study of the model has been examined. For this purpose, a microstructure with strip electrodes subjected to zero initial condition and a suddenly applied voltage with the non-dimension voltage parameter of $\lambda = 0.3$ has been considered. Fig. 2(a) and (b) shows the non-dimension midpoint deflection for non-dimension parameters of $\mu = 0$, $\gamma = 1000$ and $\hat{P}_0 = 5$ for various time increments Δt and number of elements. It can be concluded that using $\Delta t < 0.005$ and $n > 288$ results in a good convergence.

In order to validate the model, results are compared with data presented in previous researches for static pull-in parameters. The effect of Inertia and fluid pressure are ignored in equation 1 to obtain static behavior equation. Static pull-in parameters investigated in the present study using finite element method are compared with those calculated using Meshless Local Petrov Galerkin method performed by Batra et al [3] in Fig. 3 for three sample geometries: rectangular strip, annular disk and circular disk. Also dynamic pull-in parameters are calculated in the present study neglecting the effect of fluid losses and are compared with static ones in Fig. 3. Pull-in parameter λ_{pi} versus μ is shown in Fig. 3(a) for three geometries.

This figure shows the effect of scale on pull-in parameters. λ_{pi} shows the critical value of voltage and non-dimension parameter μ shows the effect of Casimir force. λ and μ depend upon device size through L^2/g_0^3 and L^2/g_0^5 respectively. Scaling down the device dimensions by a factor F ($L \rightarrow L/F$ and $g_0 \rightarrow g_0/F$) results in increase in λ by factor of F and μ by factor of F^3 . Thus as the device dimensions decrease μ increase much faster than λ . So the effect of Casimir force becomes more significant. It is obvious in Fig. 3(a) that as μ increases (decrease in system dimensions) the static and dynamic pull-in parameter λ_{pi} decreases. The intersection of curves with the horizontal axis represents the critical value of

Casimir force parameter μ_{cr} . When $\mu = \mu_{cr}$ pull-in instability occurs with no voltage applied and system collapses. This phenomenon is very important in design and fabrication process. Fig. 3 also shows the effect of inertia on pull-in parameters. It is obvious that dynamic pull-in voltage is lesser than static ones. Fig. 3(b) shows the nondimensional maximum deflection occurs when $\lambda = \lambda_{pi}$ versus μ . It is obvious that as μ increases the nondimensional maximum deflection decreases. So a reduced deflection ranges are allowable for small devices. Also it is noticeable that maximum deflection due to static pull-in is lesser than maximum deflection due to dynamic pull-in instability.



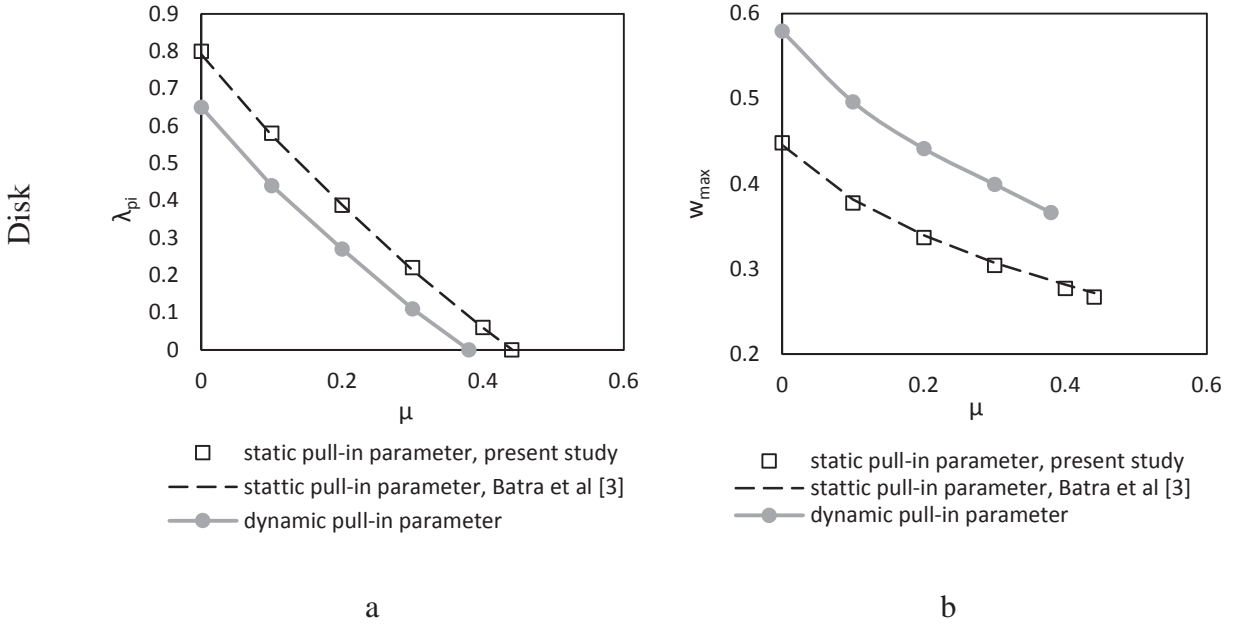


Fig. 3. (a) pull-in parameter λ_{pi} (b) maximum nondimensional deflection versus Casimir force parameter μ for three geometries

Fig. 4 shows the $\lambda_{pid}/\lambda_{pi}$ (dynamic pull-in voltage to static pull-in voltage) ratio versus Casimir force parameter μ for three geometries. Tajalli et al [22] and Krylov and Maimon [9] have calculated the ratio of dynamic pull-in voltage to static pull-in voltage for different microstructures (microplates with different lengths and initial stresses) neglecting the effect of Casimir force. They have observed that V_{pid}/V_{pi} is

almost 0.9. But fig. 4 shows the effect of Casimir force on the $\lambda_{pid}/\lambda_{pi}$ ratio. It is obvious that as μ increases (system size decreases) the $\lambda_{pid}/\lambda_{pi}$ decreases.

Phase portrait for the undamped strip structure is plotted for $\mu = 0.2$ and different non-dimension voltage parameters λ in Fig. 5. It is shown in this figure that dynamic instability occurs at $\lambda = 0.77$.

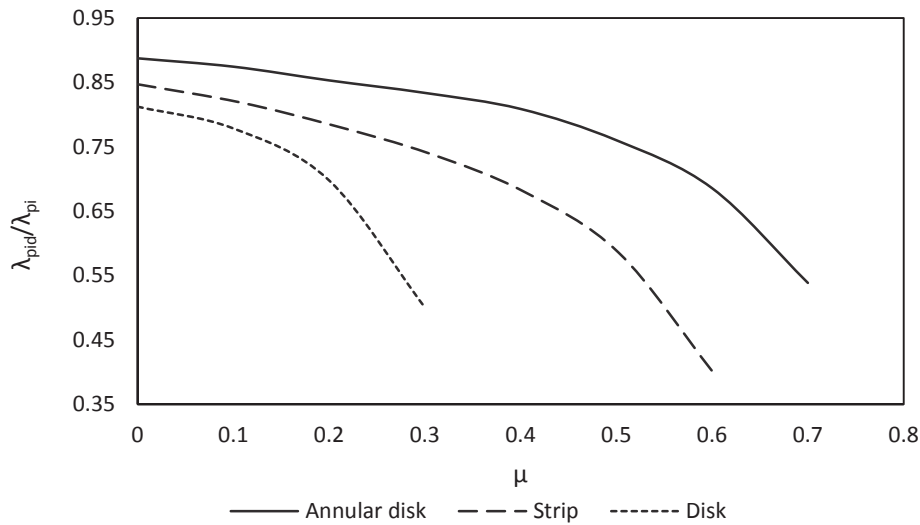


Fig. 4. $\lambda_{pid}/\lambda_{pi}$ ratio versus Casimir force parameter μ for three geometries

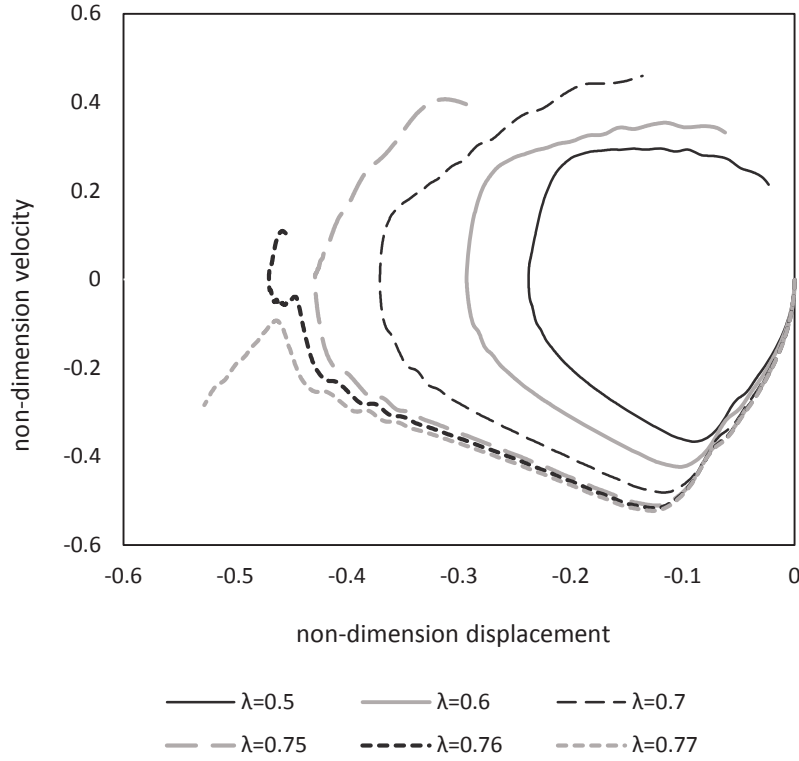


Fig. 5. Phase portrait of an undamped strip structure for $\mu = 0.2$

Midpoint deflection time history of a strip electrode for $\mu = 0.2$ is shown in Fig. 6. This figure shows that when voltage exceeds the critical value a qualitative change occurs in the dynamic behavior of system and system becomes dynamically unstable. It is obvious that for voltage parameter λ lower than its

critical value the structure performs a periodic motion while for voltage parameter higher than critical value the electrode sticks to substrate and system collapses. It is also noticeable that the oscillation amplitude increases as voltage parameter λ increases.

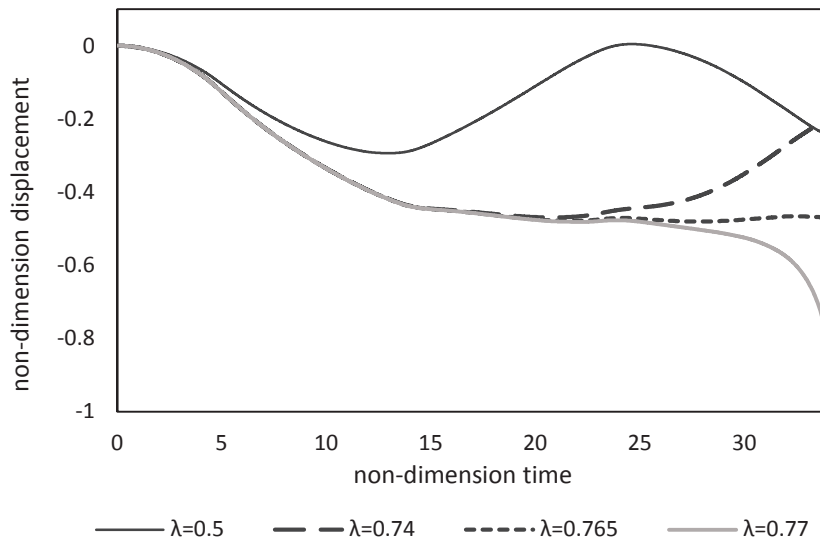


Fig. 6. Midpoint deflection time history of an undamped strip structure for $\mu = 0.2$ and different voltage parameters λ

Fig. 7 Shows the effect of squeeze film air on the dynamic behavior of the system. Casimir force effect is neglected. Midpoint deflection time history is plotted for $\lambda = 0.8$ and $\gamma = 4000$ for various non-dimension ambient pressure parameters in this figure. It is obvious that the amplitude of oscillation decreases with an increase in ambient pressure.

The effect of non-dimension parameter γ on the dynamic behavior is shown in Fig. 8. Midpoint deflection time history is plotted for various non-dimension parameter γ for $\lambda = 0.8$ and Casimir force effect is neglected. This figure shows that as γ increases maximum overshoot of vibration decreases but the oscillations would be damped later.

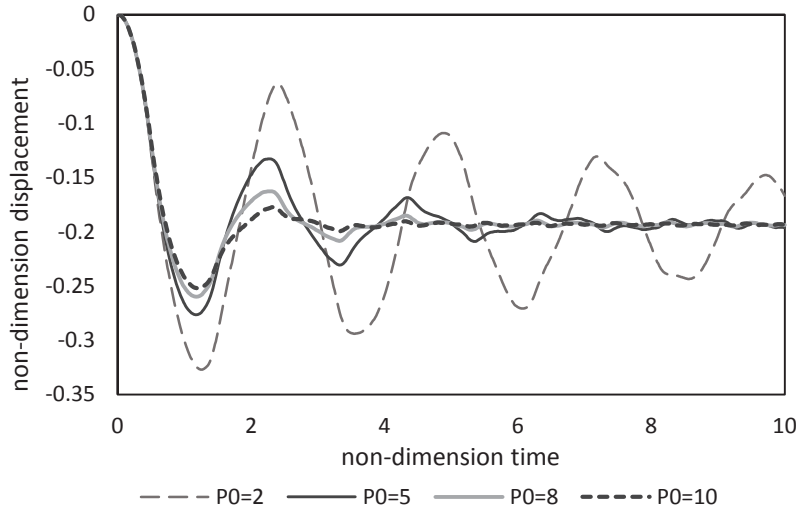


Fig. 7. Midpoint deflection time history of a strip membrane for various ambient pressure non-dimension parameters for $\lambda = 0.8$ and $\mu = 0$

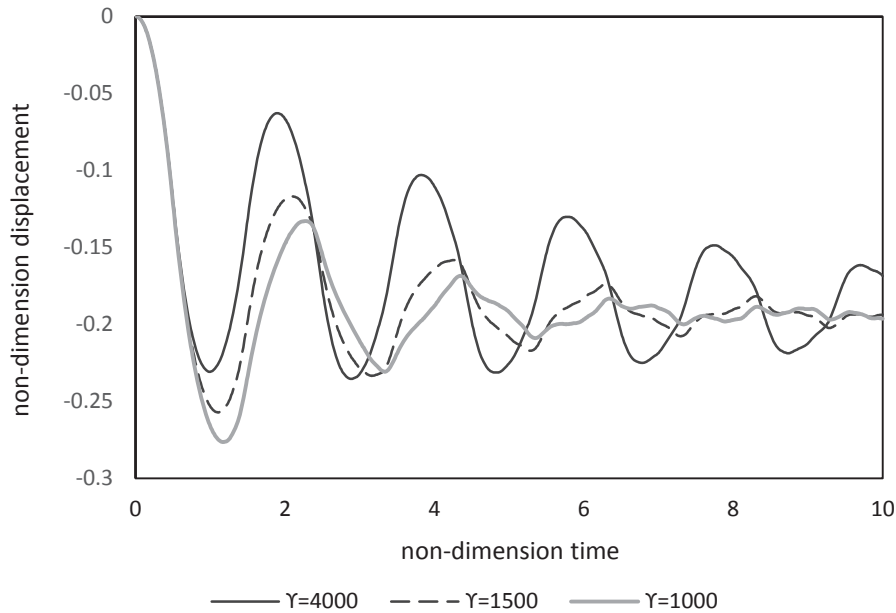


Fig. 8. Midpoint deflection time history of a strip membrane for $\lambda = 0.8$ and $\mu = 0$ for various non-dimension parameters γ

In Fig. 9 the response of a strip microstructure to suddenly applied voltage considering the effect of

squeeze film air damping is shown. The effect of Casimir force is ignored. Midpoint deflection time history is plotted for $\gamma = 4000$ and $\hat{P}_0 = 5$ for various

voltage parameters λ . It is obvious that as λ increases, the amplitude of vibrations and the amplitude of steady-state motion increase.

5. Conclusions

The main idea of the present study was to model MEMS and NEMS using linear elastic membrane theory. In this study, the effect of Casimir force and squeeze film air on the static and dynamic pull-in instability and dynamic behavior of system has been investigated. Fluid losses were modeled using nonlinear Reynolds equation. Finite element method was applied to discretize and solve the governing

equations for three considered geometries. Results showed that as the device sizes decrease, the effect of Casimir force becomes more important. There is a minimum size for device in the fabrication process at which system collapses without applying any voltage. Also the effect of system size and Casimir force on V_{pid}/V_{pi} ratio has been investigated. It has been observed that with a decrease in system sizes the ratio of dynamic pull-in voltage to static pull-in voltage decreases. Results showed the significant effect of squeeze film air and ambient pressure on the dynamic behavior of membrane-based MEMS.

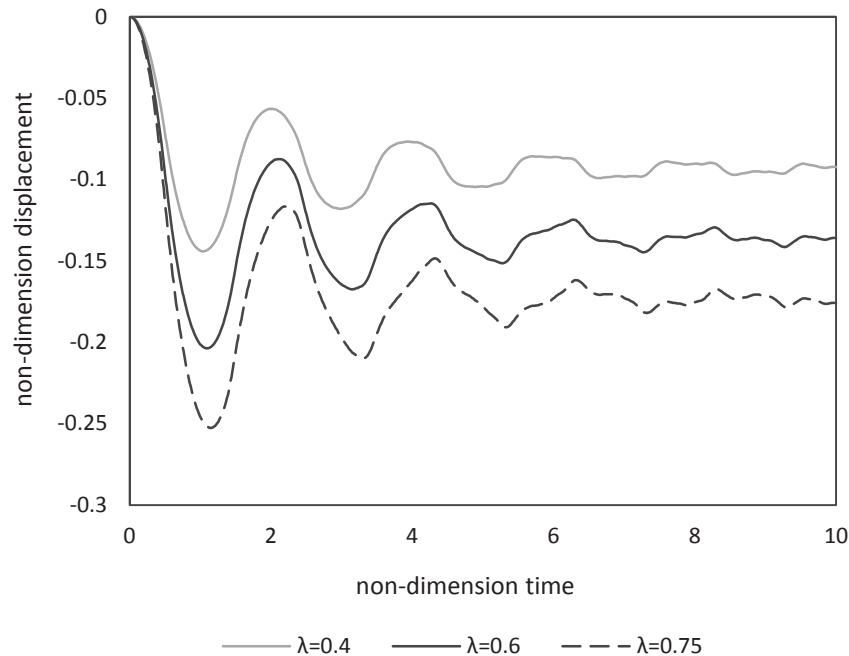


Fig. 9. Midpoint deflection time history for $\gamma = 4000$ and $\hat{P}_0 = 5$ for various voltage parameters λ

References

- [1] H. C. Nathanson, W. E. Newell, R. A. Wickstrom, J. R. Davis Jr, The resonant gate transistor, *Electron Devices, IEEE Transactions on*, Vol. 14, No. 3, pp. 117-133, 1967.
- [2] G. Taylor, The coalescence of closely spaced drops when they are at different electric potentials, in *Proceeding of*, The Royal Society, pp. 423-434.
- [3] R. Batra, M. Porfiri, D. Spinello, Effects of Casimir force on pull-in instability in micromembranes, *EPL (Europhysics Letters)*, Vol. 77, No. 2, pp. 20010, 2007.
- [4] H. Moeenfarid, A. Darvishian, M. T. Ahmadian, Modeling of pull-in instability of nano/micromirrors under the combined effect of capillary and casimir forces, *International Journal of Optomechatronics*, Vol. 5, No. 4, pp. 378-392, 2011.
- [5] M. Dequesnes, S. Rotkin, N. Aluru, Calculation of pull-in voltages for carbon-nanotube-based nanoelectromechanical switches, *Nanotechnology*, Vol. 13, No. 1, pp. 120, 2002.
- [6] H. A. Tilmans, R. Legtenberg, Electrostatically driven vacuum-encapsulated polysilicon resonators: Part II. Theory and performance, *Sensors and Actuators A: Physical*, Vol. 45, No. 1, pp. 67-84, 1994.
- [7] H. Sadeghian, Surface stress effects on the electrostatic pull-in instability of

- nanomechanical systems, *arXiv preprint arXiv:1611.02222*, 2016.
- [8] F. M. Alsaleem, M. I. Younis, H. M. Ouakad, On the nonlinear resonances and dynamic pull-in of electrostatically actuated resonators, *Journal of Micromechanics and Microengineering*, Vol. 19, No. 4, pp. 045013, 2009.
- [9] S. Krylov, R. Maimon, Pull-in dynamics of an elastic beam actuated by continuously distributed electrostatic force, *Journal of vibration and acoustics*, Vol. 126, No. 3, pp. 332-342, 2004.
- [10] M. Moghimi Zand, M. T. Ahmadian, Dynamic pull-in instability of electrostatically actuated beams incorporating Casimir and van der Waals forces, *Proceedings of the Institution of Mechanical Engineers, Part C: Journal of Mechanical Engineering Science*, Vol. 224, No. 9, pp. 2037-2047, 2010.
- [11] M. Moghimi Zand, M. T. Ahmadian, Application of homotopy analysis method in studying dynamic pull-in instability of microsystems, *Mechanics Research Communications*, Vol. 36, No. 7, pp. 851-858, 2009.
- [12] H. Daneshpajooh, M. Moghimi Zand, Semi-analytic solutions to oscillatory behavior of initially curved micro/nano systems, *Journal of Mechanical Science and Technology*, Vol. 29, No. 9, pp. 3855-3863, 2015.
- [13] M. Moghimi Zand, M. Ahmadian, B. Rashidian, Semi-analytic solutions to nonlinear vibrations of microbeams under suddenly applied voltages, *Journal of Sound and Vibration*, Vol. 325, No. 1, pp. 382-396, 2009.
- [14] A. H. Nayfeh, M. I. Younis, Dynamics of MEMS resonators under superharmonic and subharmonic excitations, *Journal of Micromechanics and Microengineering*, Vol. 15, No. 10, pp. 1840, 2005.
- [15] M. Moghimi Zand, M. Ahmadian, Vibrational analysis of electrostatically actuated microstructures considering nonlinear effects, *Communications in Nonlinear Science and Numerical Simulation*, Vol. 14, No. 4, pp. 1664-1678, 2009.
- [16] M. Weinberg, R. Candler, S. Chandorkar, J. Varsanik, T. Kenny, A. Duwel, Energy loss in MEMS resonators and the impact on inertial and RF devices, *Proc. Transducers 2009*, pp. 688-695, 2009.
- [17] A. K. Pandey, R. Pratap, Effect of flexural modes on squeeze film damping in MEMS cantilever resonators, *Journal of Micromechanics and Microengineering*, Vol. 17, No. 12, pp. 2475, 2007.
- [18] B. McCarthy, G. G. Adams, N. E. McGruer, D. Potter, A dynamic model, including contact bounce, of an electrostatically actuated microswitch, *Microelectromechanical Systems, Journal of*, Vol. 11, No. 3, pp. 276-283, 2002
- [19] M. I. Younis, *Modeling and simulation of microelectromechanical systems in multi-physics fields*, Thesis, Citeseer, 2004..
- [20] M. I. Younis, A. H. Nayfeh, Simulation of squeeze-film damping of microplates actuated by large electrostatic load, *Journal of Computational and Nonlinear Dynamics*, Vol. 2, No. 3, pp. 232-241, 2007.
- [21] P. Y. Kwok, M. S. Weinberg, K. S. Breuer, Fluid effects in vibrating micromachined structures, *Microelectromechanical Systems, Journal of*, Vol. 14, No. 4, pp. 770-781, 2005.
- [22] S. Tajalli, M. Moghimi Zand, M. Ahmadian, Effect of geometric nonlinearity on dynamic pull-in behavior of coupled-domain microstructures based on classical and shear deformation plate theories, *European Journal of Mechanics-A/Solids*, Vol. 28, No. 5, pp. 916-925, 2009.
- [23] M. Bao, H. Yang, Y. Sun, P. J. French, Modified Reynolds' equation and analytical analysis of squeeze-film air damping of perforated structures, *Journal of Micromechanics and Microengineering*, Vol. 13, No. 6, pp. 795, 2003.
- [24] D. Yan, A. Lal, The squeeze film damping effect of perforated microscanners: modeling and characterization, *Smart materials and structures*, Vol. 15, No. 2, pp. 480, 2006.
- [25] J. B. Starr, Squeeze-film damping in solid-state accelerometers, in *Proceeding of, IEEE*, pp. 44-47.
- [26] M. J. Martin, B. H. Houston, J. W. Baldwin, M. K. Zalalutdinov, Damping models for microcantilevers, bridges, and torsional resonators in the free-molecular-flow regime, *Microelectromechanical Systems, Journal of*, Vol. 17, No. 2, pp. 503-511, 2008.
- [27] S. Hutcherson, W. Ye, On the squeeze-film damping of micro-resonators in the free-molecule regime, *Journal of Micromechanics*

- and *Microengineering*, Vol. 14, No. 12, pp. 1726, 2004.
- [28] A. Alipour, M. Moghimi Zand, H. Daneshpajooh, Analytical solution to nonlinear behavior of electrostatically actuated nanobeams incorporating van der Waals and Casimir forces, *Scientia Iranica*, Vol. 22, No. 3, pp. 1322-1329, 2015.
- [29] A. Koochi, A. S. Kazemi, Y. T. Beni, A. Yekrangi, M. Abadyan, Theoretical study of the effect of Casimir attraction on the pull-in behavior of beam-type NEMS using modified Adomian method, *Physica E: Low-dimensional Systems and Nanostructures*, Vol. 43, No. 2, pp. 625-632, 2010.
- [30] M. Keivani, J. Khorsandi, J. Mokhtari, A. Kanani, N. Abadian, M. Abadyan, Pull-in instability of paddle-type and double-sided NEMS sensors under the accelerating force, *Acta Astronautica*, Vol. 119, pp. 196-206, 2016.
- [31] W.-H. Lin, Y.-P. Zhao, Nonlinear behavior for nanoscale electrostatic actuators with Casimir force, *Chaos, Solitons & Fractals*, Vol. 23, No. 5, pp. 1777-1785, 2005.
- [32] A. Ramezani, A. Alasty, J. Akbari, Analytical investigation and numerical verification of Casimir effect on electrostatic nano-cantilevers, *Microsystem Technologies*, Vol. 14, No. 2, pp. 145-157, 2008.
- [33] G. Xie, J. Ding, S. Liu, W. Xue, J. Luo, Interfacial properties for real rough MEMS/NEMS surfaces by incorporating the electrostatic and Casimir effects—a theoretical study, *Surface and Interface Analysis*, Vol. 41, No. 4, pp. 338-346, 2009.
- [34] Y. T. Beni, A. Koochi, M. Abadyan, Theoretical study of the effect of Casimir force, elastic boundary conditions and size dependency on the pull-in instability of beam-type NEMS, *Physica E: Low-dimensional Systems and Nanostructures*, Vol. 43, No. 4, pp. 979-988, 2011.
- [35] J. Duan, Z. Li, J. Liu, Pull-in instability analyses for NEMS actuators with quartic shape approximation, *Applied Mathematics and Mechanics*, Vol. 37, No. 3, pp. 303-314, 2016.
- [36] Y. Tadi Beni, F. Mehralian, The effect of small scale on the free vibration of functionally graded truncated conical shells, *Journal of Mechanics of Materials and Structures*, Vol. 11, No. 2, pp. 91-112, 2016.
- [37] Y. G. Wang, H. F. Song, W. H. Lin, Nonlinear Pull-In Characterization of a Nonlocal Nanobeam with an Intermolecular Force, *Journal of Mechanics*, pp. 1-11, 2016.
- [38] A. Kanani, A. Koochi, M. Farahani, E. Rouhic, M. Abadyan, Modeling the size dependent pull-in instability of cantilever nano-switch immersed in ionic liquid electrolytes using strain gradient theory, *Scientia Iranica. Transaction B, Mechanical Engineering*, Vol. 23, No. 3, pp. 976, 2016.
- [39] S. Saghir, M. I. Younis, Approaches for Reduced-Order Modeling of Electrically Actuated von-Karman Microplates, *Journal of Computational and Nonlinear Dynamics*, Vol. 12, No. 1, pp. 011011, 2017.
- [40] F. M. Serry, D. Walliser, G. J. Maclay, The role of the Casimir effect in the static deflection and stiction of membrane strips in microelectromechanical systems (MEMS), *Journal of Applied Physics*, Vol. 84, No. 5, pp. 2501-2506, 1998.
- [41] E. Ventsel, T. Krauthammer, 2001, *Thin plates and shells: theory: analysis, and applications*, CRC press,
- [42] T. Veijola, H. Kuisma, J. Lahdenperä, T. Ryhänen, Equivalent-circuit model of the squeezed gas film in a silicon accelerometer, *Sensors and Actuators A: Physical*, Vol. 48, No. 3, pp. 239-248, 1995.